Electronic structure of dense amorphous carbon

Choon H. Lee,* Walter R. L. Lambrecht, and Benjamin Segall
Department of Physics, Case Western Reserve University, Cleveland, Ohio 44106-7079

Pantelis C. Kelires
Physics Department, University of Crete and Research Center of Crete, P. O. Box 1527, 71110 Heraklion, Crete, Greece

Thomas Frauenheim and Uwe Stephan
Department of Physics, Technical University of Chemnitz-Zwickau, D-09009 Chemnitz, PSF 964, Germany
(Received 10 January 1994)

The tight-binding method is used to calculate the electronic densities of states of various models of a-C. Both models generated using Tersoff's potential and quantum mechanically derived forces show π and π^* states in the σ gap in agreement with experimental data. The former models, however, have an additional large peak at the Fermi level, which is shown to derive mainly from misoriented p_π orbitals and dangling bonds. The models do not support the presence of large aromatic ring structures. We find that embedding the local π electron systems of small clusters in the rigid sp^3 network leads to reduced level splittings and is thus consistent with the observed small optical gaps ≤ 2.5 eV.

The structure of dense and hard a-C films, often called diamondlike carbon (DLC) is still controversial. For an overview of a-C properties and deposition techniques, see Ref. 1. In this paper, we focus on hydrogen-free films of the type produced by laser ablation or high-energy ion-beam deposition[2] on highly conductive substrates and vacuum-arc generated mass-selected ion-beam (MSIB) deposition.[3] Studies of the radial distribution function by neutron diffraction[4] and electron energy loss spectroscopy (EELS) (Refs. 2 and 5) have suggested a large fraction of sp^3 bonds, as high as 90%, for this form of carbon. Here, we present a comparative study of the electronic structure of different models[6,7] for this material. Our main findings are that (1) semiempirical potential models[6] have adequate clustering of threefold sites but lead to an excessive number of states at E_F due to a lack of local bond rearrangements favoring π bonding; (2) contrary to an existing theory,[8] aromatic structures are not needed to explain the small optical gaps and not supported by either set of models.

Recently, Kelires[6] generated models of a-C by means of a Monte Carlo method and the semiempirical Tersoff potential.[9] While models generated at low pressure, referred to as e-C (e for evaporated) had $\sim$ 90% threefold sites, high pressure led to models (i-C) (i for ion beam) with $\sim$70–90 % fourfold sites. The high pressure can be thought of as representing the local stresses generated in the films under high-energy ion deposition conditions.[10] However, it was found that many of the fourfold sites are in a state of high local stress. Upon annealing, this state relaxes to an sp^2-rich phase denoted as i-C*, which, however, roughly maintains the high density and bulk modulus of i-C. Evidence that cross-linked sp^2 sites contribute to rigidity can be derived from the hardness of magnetron sputtered a-C.[1] The mechanical properties are macroscopic averages and thus do not provide a stringent test of the microscopic structure. Apparently, high bulk moduli and densities can be obtained from models which are rather different in their sp^2 content and local structure. A more stringent test is provided by the electronic structure which, for example, can be compared to EELS and optical absorption data.

Here, we use the tight-binding method to calculate the electronic densities of states of the models produced in Ref. 6. The parameters in our semiempirical tight-binding Hamiltonian were adjusted so as to give a fairly accurate band structure for both graphite and diamond and the ideal diamond {111} surface with and without hydrogen. Details are given in Ref. 11. Here we just note that the bandwidths of diamond and of the σ and π bands of graphite and their relative position are well reproduced. Also, a dangling bond in the middle of the gap is correctly obtained for the ideal diamond {111} surface. Because of the limitation to nearest neighbor interactions, the band gap of diamond, however, comes out to be direct at the Γ point. On the other hand, this higher direct band gap compensates for the underestimate due to the local density approximation. Thus, our effective band gap for diamond is $\sim$5 eV, in close agreement with experiment. For graphite, the splitting of the π-state maxima in the density of states corresponding to the M-critical point is $\sim$6 eV instead of $\sim$4 eV. Because both of these shortcomings are related to long-range order, we believe that they are not too important for our present study of a-C. Standard diagonalization methods are applicable because the models have periodic boundary conditions. The densities of states of the a-C models are calculated by summing over four special k points.

The structural properties of the models are summarized in Table I. The i-C model does not have any clusters larger than pairs. The i-C* model has mostly larger clusters of sp^2 sites but only a small number of closed

TABLE I. Structural properties of the models.

Percentages[a]	i-C	i-C*	e-C	F-MD
fourfold	72	28	11	51
threefold	28	70	84	47
twofold	0	2	5	2
isolated	50	5	0	7
in isolated pairs	50	3	0	13
in larger clusters	0	92	100	80
density (g/cm^3)	3.2	2.9	2.0	3.0
average bond length (Å)	1.53	1.48	1.47	1.52

[a]First three rows: % of total; next three rows: % of threefold.

rings consisting purely of sp^2 sites and no odd-membered rings at all. Most of the rings contain both sp^2 and sp^3 atoms and are not flat. No regions of fused flat sixfold rings are present. Although this is not surprising for i-C with a sp^3 site concentration of up to 90%, it is also true for i-C* and e-C and conflicts with models proposed by Robertson and O'Reilly[8] and Tamor and Wu.[12] In those models, the presence of fairly large graphitic regions is postulated in order to explain the occurrence of a rather small optical gap in a-C and a-C:H films (0.5–2.0 eV).

The results for densities of states (DOS) are shown in Fig. 1. The DOS of panel (a) is for the fully fourfold coordinated 216-atom Wooten-Winer-Weaire model (WWW)

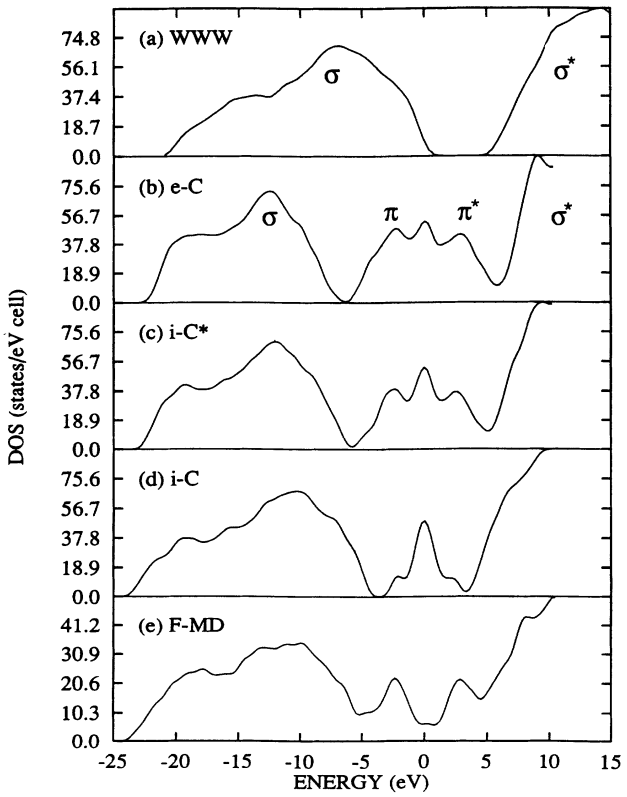

FIG. 1. Densities of electronic states for (a) the WWW model of Ref. 13, adapted for C as described in Ref. 11, (b) e-C, (c) i-C*, and (d) i-C models of Ref. 6, and (e) a-C of Ref. 7. The σ, σ^*, π, π^* peaks referred to in the text are indicated. The Fermi energy is at zero.

suitably adapted[11] to C.[13] We see that in contrast to the WWW model, the three models generated by the Monte Carlo method [shown in panels (b)-(d)] have a broad distribution of π bonding and antibonding states as well as a significant density of states near the Fermi level E_F in the gap between σ and σ^* bands. We also note that the σ-state valence band DOS becomes narrower and the σ gap widens from the WWW to i-C to i-C* to e-C model, i.e., with decreasing sp^3 content. This is consistent with the stronger in-plane σ bonds in sp^2-bonded carbon. The DOS in the σ gap of the i-C model has a high peak at E_F with only small "wings" of π-bonding states. The increase in π peaks in the i-C* model is consistent with the significantly reduced number of isolated sites. However, Table I indicates that the states at E_F cannot be exclusively attributed to isolated sites. In fact, there are very few isolated threefold sites in the i-C* and e-C models. To elucidate the origin of the states at E_F, we note that p_π orbitals (i.e., p orbitals perpendicular to the local sp^2 plane) at neighboring sp^2 sites only form π bonds effectively if they are nearly parallel. For orbitals oriented relative to each other by a dihedral angle θ, the π interaction is reduced by $\cos\theta$. For a random distribution of θ, $x = \cos\theta$ has a $1/\sqrt{1-x^2}$ distribution, which would still predict a two peaked density of the corresponding electronic states. However, a lack of coplanarity of the sp^2 orbitals implies a rehybridization towards sp^3, which leads to a third peak at E_F. The states at E_F are thus intermediate in character between sp^3 "dangling bonds" and lone-pair p states and indicate that the threefold sites are generally not truly sp^2-like. See Stephan and Haase[14] for further discussion of topological π defects.

The total number of states in the σ gap increases from i-C to i-C* to e-C. This means that sp^3 sites were converted into sp^2 sites, in agreement with the statistics of Table I and consistent with the annealing mechanism described in Ref. 6. The slightly increasing average π-π^* splitting from i-C to i-C* to e-C is consistent with the decrease in average bond length. The total number of states in the σ gap irrespective of whether they occur at E_F or as π or π^* states is in closer agreement with experiments on MSIB carbon[5] for i-C than for i-C*. That i-C is a better model for as-formed MSIB carbon was also concluded from a detailed comparison of the structure factor.[15] The i-C* model, however, may be relevant to high-temperature annealed MSIB carbon.

Models generated by molecular dynamics (MD) using quantum mechanically calculated forces[7,16,17] do not show a peak at E_F. To ensure that the peak at E_F for the Tersoff models is not due to an artifact of our tight-binding (TB) Hamiltonian, we used it to calculate the DOS for a 3.0 g/cm^3 model of 128 atoms produced by Frauenheim *et al.*[7] using an approximate local density approximation scheme and molecular dynamics (LDA-MD). The present work is denoted F-MD. The result in panel (e) of Fig. 1 shows only a small DOS at E_F, in good agreement with the corresponding LDA results published in Fig. 12 of Ref. 7. The π and π^* peak positions, however, are similar to those in Kelires's models. We next compare both models' distribution of π states to experiment.

The strong peak in DOS near E_F is in conflict with the high resistivity of DLC, with the existence of an optical gap and the absence of a signature from states at E_F in carbon-K-edge and low-energy EELS spectra. Carbon-K-edge EELS gives information on the separation of the π^* state from the inflection point of the σ^* band onset. These spectra in the near-edge region are dominated by the transitions from the C($1s$) level to unoccupied states and thus give information on the lowest unoccupied DOS. The measured π^*-σ^* separation is 6.1 eV in graphite, 5 eV in typical a-C, and 3.4 eV in MSIB carbon. While the π^* peak is about equally intensive in typical (low-energy deposition) a-C and in graphite, it is 3–5 times weaker in MSIB carbon.[2,5] We find for this splitting 5 eV for e-C and graphite, 4.5 eV for i-C*, and 3 eV for i-C, in fair agreement with the experimental trend. Intensities are more difficult to compare because of matrix-element effects, but appear reasonable.

The peak in the low-energy EELS at 4.8 eV in a-C and 6.2 eV in graphitized carbon[5] is associated with $\pi \rightarrow \pi^*$ transitions, sometimes termed a π plasmon.[18,19] It was also observed in the films made by Cuomo *et al.*[2] In graphite, the 6 eV peak in the loss function $-\mathrm{Im}\,\epsilon^{-1}$ is associated with a peak at 4 eV in $\epsilon_2(\omega)$ (Ref. 20) corresponding to a critical point transition at M. Similar peak shifts between the loss function and $\epsilon_2(\omega)$ obtained from it by Kramers-Kronig analysis were obtained for a-C:H by Fink *et al.*[21] We would thus expect the loss feature to occur at slightly higher energy than our calculated peak splittings. On the other hand, our TB Hamiltonian overestimates the M critical point transition in graphite, as mentioned earlier. There may thus be some compensation of these two effects. We find $\pi - \pi^*$ splittings of 6 eV, 5 eV, and 4 eV for e-C, i-C* (and F-MD), and i-C, respectively, in satisfactory agreement with the data. We note that in MSIB carbon the π-π^* transition could not be detected in low-energy EELS,[5] while the π^* peak was detected in K-edge EELS. This is consistent with the electronic structure of a 64-atom model with 83% sp^3 and $\rho = 3.3$ g/cm^3 generated by LDA MD,[7] in which the π states merge with the broader σ valence band while the π^* remains clearly visible in the gap.

To further investigate the nature of the π and E_F states, we have performed separate calculations of the local (L)DOS of models with specific clusters of sp^2 sites, embedded in an otherwise fully fourfold coordinated network represented by the WWW model.[13] These sites were created by breaking bonds and relaxing the structure to a local minimum with the Tersoff potential and a static variable metric relaxation method.[11] These LDOS (shown in Fig. 2) indicate that the π-π^* splitting is ~5.1 eV for a pair of π-bonded sp^2 sites, ~3.1 eV for a typical triplet, and ~1.7 eV for a hexagonal ring.

In the case of the triplet [panel (b)], a peak is obtained at E_F. Examination of the local configuration reveals that this triplet is better described as a pair of sp^2 sites linked to an "sp^3-hybridized" dangling bond site. Indeed, the peak at E_F is mostly centered on the atom on the right and has a significant s contribution. One also sees that the sp^2 planes of the pair are not quite parallel and this accounts for the reduced splitting of the π-π^* peaks. Similar effects of local distortions were noted on other local configurations and provide evidence for our interpretation of the origin of the states at E_F given above.

The spectrum of the hexagon model [panel (c)] can be viewed as a modification of the four level spectrum of benzene [-2β (1), $-\beta$ (2), β (2), and 2β (1), with the number in parentheses being the degeneracy]. Because the embedded hexagon is not exactly planar and does not have all bond lengths equal, the degeneracy of the two inner peaks is lifted. The characteristic splitting is $\beta \approx$ 1.8 eV instead of the ~3 eV for molecular benzene. The degeneracy lifting further reduces the gap. This shows that even for a *single* hexagon of sp^2 sites a gap ≤ 2 eV can be obtained. We note that there is a considerable spread of the characteristic splittings of the embedded molecular fragments. For example, another hexagonal fragment gave a local gap of ~ 3 eV.

The reduction of the splitting from that in the isolated molecules is attributed to the effects of the embedding. The latter leads to distortions in local bond lengths, dihedral distortions, and distortions from the local planarity or linearity of the molecular fragments. This leads to coupling between the π- and σ-electronic systems and to delocalization of the π-electronic states to the surrounding medium. This effectively reduces or renormalizes the π interactions in a manner reminiscent of the reduction of the Coulomb interaction between different

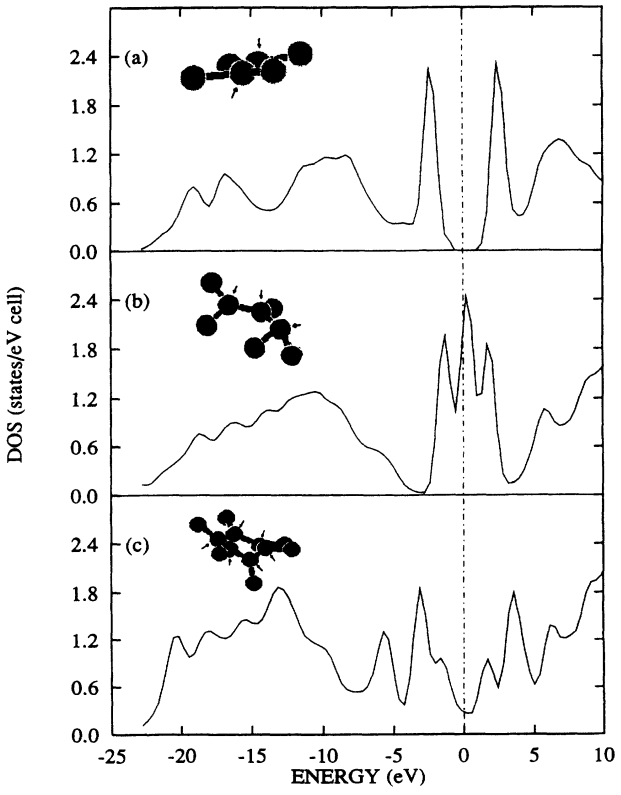

FIG. 2. Local densities of states for (a) a pair, (b) a triplet, and (c) a hexagon of π-bonded neighboring sp^2 sites embedded in the WWW model. The local atomic configurations are shown as insets. The LDOS is a sum over the atoms indicated by arrows.

charge states of an impurity embedded in a semiconductor in the Haldane-Anderson model.[22]

The effective optical gap is determined by the smallest π-π^* splitting which occurs with non-negligible abundance and not by the most predominant splitting. The rather large π-π^* average peak splitting in all the models indicates that the majority of the p_π orbitals only participate in small π bonding groupings. In the larger clusters lone pair p orbitals and dangling bonds usually interrupt the conjugation of π electrons. This is consistent with the insulating character of materials with high sp^3 content. Although there is clustering of sp^2 sites driven by π-bonding stabilization in the Frauenheim models, the equally occurring fivefold, sixfold, and sevenfold rings are strongly cross linked by inclusion of at least one or two sp^3 sites. They are, thus, not aromatic. In MSIB C, the occurrence of a separate (and aromatic) sp^2 phase is very difficult to envision because the sp^2 concentration is only 10–15 %. Both types of models studied here indicate the absence of aromatic regions even in lower density a-C. The LDA-MD calculations indicate that this also holds true in hydrogenated a-C:H.[7]

In conclusion, both Tersoff-potential and LDA derived models of a-C have electronic structures in fair agreement with experimental EELS data except that the Tersoff-potential models have too large a density of defect states at E_F. The latter is primarily due to incorrect hybridization (too much sp^3-like even at threefold sites) and dihedral disorder and not to a lack of clustering of threefold sites. The previously postulated existence of extended aromatic regions is not supported by the models. In addition, it is found to be unnecessary to explain the small gaps when the embedding effects on local molecular structures is taken into account.

We are grateful to Dr. K. Winer for providing the coordinates of the WWW model and to Dr. A. T. Paxton for use of his tight-binding program. The authors at C.W.R.U. acknowledge support by the National Science Foundation (Grant No. DMR-91-21479) and the use of the Ohio Supercomputer Center. Finally, we thank Professor J. C. Angus for his interest in our work.

---

*Present address: Department of Physics and Center for Thermal and Statistical Physics, Korea University, Seoul 136-701, Korea.

[1] J. Robertson, Adv. Phys. **35**, 317 (1986); Surf. Coat. Technol. **50**, 185 (1992); Diamond Relat. Mater. **1**, 297 (1992).

[2] J. J. Cuomo, D. L. Pappa, J. Bruley, J. P. Doyle, and K. L. Saenger, J. Appl. Phys. **70**, 1706 (1991); J. J. Cuomo, J. P. Doyle, J. Bruley, and J. C. Liu, J. Vac. Sci. Technol. A **9**, 2210 (1991).

[3] D. R. McKenzie, D. C. Green, P. D. Swift, D. J. H. Cockayne, P. J. Martin, R. P. Netterfield, and W. G. Sainty, Thin Solid Films **193**, 418 (1990).

[4] P. H. Gaskell, A. Saeed, P. Chieux, and D. R. McKenzie, Phys. Rev. Lett. **67**, 1286 (1991).

[5] S. D. Berger, D. R. McKenzie, and P. J. Martin, Philos. Mag. B **52**, 285 (1988)

[6] P. C. Kelires, Phys. Rev. Lett. **68**, 1854 (1992); Phys. Rev. B **47**, 1829 (1993); (unpublished).

[7] Th. Frauenheim, P. Blaudeck, U. Stephan, and G. Jungnickel, Phys. Rev. B **47**, 4823 (1993); P. Blaudeck, Th. Frauenheim, D. Porezag, G. Seifert, and E. Fromm, J. Phys. Condens. Matter **4**, 6389 (1992).

[8] J. Robertson and E. P. O'Reilly, Phys. Rev. B **35**, 2946 (1987).

[9] J. Tersoff, Phys. Rev. Lett. **61**, 2879 (1988).

[10] D. R. McKenzie, D. Muller, and B. A. Pailthorpe, Phys. Rev. Lett. **67**, 773 (1991).

[11] C. H. Lee, Ph.D. thesis, Case Western Reserve University, 1993.

[12] M. A. Tamor and C. H. Wu, J. Appl. Phys. **67**, 1007 (1990); M. A. Tamor, J. A. Haire, C. H. Wu, and K. C. Hass, Appl. Phys. Lett. **54**, 123 (1989).

[13] F. Wooten, K. Winer, and D. Weaire, Phys. Rev. Lett. **54**, 1392 (1985).

[14] U. Stephan and M. Haase, J. Phys. Condens. Matter **5**, 9157 (1993).

[15] P. Kelires, C. H. Lee, and W. R. Lambrecht, J. Non-Cryst. Solids **164-166**, 1131 (1993).

[16] G. Galli, R. M. Martin, R. Car, and M. Parinello, Phys. Rev. Lett. **62**, 555 (1989); Phys. Rev. B **42**, 7470 (1990).

[17] C. Z. Wang, K. M. Ho, and C. T. Chan, Phys. Rev. Lett. **70**, 611 (1993).

[18] P. G. Lurie and J. M. Wilson, Surf. Sci. **65**, 476 (1977).

[19] Y. Wang, H. Chen, R. W. Hoffman, and J. C. Angus, J. Mater. Res. **5**, 2378 (1990).

[20] E. A. Taft and H. R. Philipp, Phys. Rev. **138**, A197 (1965).

[21] J. Fink, Th. Müller-Heinzerling, J. Pflüger, B. Scheerer, B. Dischler, P. Koidl, A. Bubenzer, and R. E. Sah, Phys. Rev. B **30**, 4713 (1984).

[22] F. D. M. Haldane and P. W. Anderson, Phys. Rev. B **13**, 2553 (1976).